Harmonic Control for Variable-Frequency Aviation Power System Based on Three-Level NPC Converter

ZHENYANG HAO[ID], **(Member, IEEE), XINYING WANG**[ID]**, AND XIN CAO**[ID]**, (Member, IEEE)**
Department of Electrical Engineering, Nanjing University of Aeronautics and Astronautics, Nanjing 210016, China

Corresponding author: Zhenyang Hao (zhenyang_hao@nuaa.edu.cn)

ABSTRACT At present, three-phase 115V/360-800Hz variable frequency AC power system is mostly used in the main power system of More-Electric Aircraft. With the increase of EMA (Electro-Mechanical Actuator), EHA (Electro-Hydrostatic Actuator), DC/DC power supply and power electronic devices in More-Electric Aircraft, harmonic and reactive power problems are brought, which seriously affect the power supply quality of variable frequency power supply for aircraft. According to the characteristics of high frequency and wide range of aviation variable frequency power supply, this paper studies a three-level active filter which can effectively improve the power quality of aviation variable frequency power supply system. This paper analyzes the working principle of the diode clamped three-level topology active filter, and deduces its mathematical model; proposes the frequency detection of the aviation variable frequency power supply based on the improved Rife method; the ip-iq method based on the instantaneous reactive power theory, accurately detects the harmonic current of the aviation variable frequency power supply system; uses the quasi PR controller to track the current, and improves the harmonic suppression effect. Finally, the experimental hardware platform is built to verify the feasibility of the proposed control strategy.

INDEX TERMS Aviation variable frequency power supply, active power filter, frequency detection, harmonic current detection, quasi PR control.

I. INTRODUCTION

With the rapid development of aviation technology, the frequency of airborne electronic equipment is higher and higher, which makes the problem of harmonic, reactive power and voltage imbalance more and more serious, so it affects the power supply quality of aircraft power supply system. Aviation power supply system, which means the generation, transformation, transmission and distribution of electric energy on the aircraft, is divided into two parts: power supply system and power transmission and distribution system [1]. There are three kinds of modern air-craft power system: DC power, AC power and hybrid power. Among them, DC power supply has high and low voltage, namely 270V, 28.5V. AC power supply includes constant speed constant frequency, variable speed constant frequency and variable speed variable frequency system. At present, most aircraft require uninterrupted power supply, so the new generation hybrid power supply is more suitable for More-Electric Aircraft.

The associate editor coordinating the review of this manuscript and approving it for publication was Norbert Herencsar[ID].

For the aviation variable frequency power supply system, it is required to work reliably with low cost [1], at the same time, it can provide better power quality and low weight. Among them, the harmonic problem is an important reason that affects the quality of power supply. The power quality of Aircraft AC power supply has voltage, frequency, current and other indicators. In the national military standard GJB 181B-2012, the current distortion is specified as follows: all electrical equipment shall not introduce excessive current distortion that can affect other equipment. Unless otherwise specified, the current distortion coefficient of AC electrical equipment shall not be greater than 10%. However, in practical application, harmonics are often introduced into every link, which affects the power quality and normal operation of the equipment. In the power generation process, the generator and frequency converter will introduce harmonics; in the power distribution system, the corresponding rectifiers will also introduce a large number of harmonics, resulting in the degradation of power quality; in the load, that is, in the airborne equipment, lighting and heating equipment, arc furnace and other gas light sources are all harmonic sources.

There are two methods to solve harmonic problems, active method and passive method. Active control can be understood as reducing the generation of harmonics for those devices that generate harmonics, such as the transformation of non-linear devices, so that non-linear devices no longer generate harmonics. Active control can adopt multi pulse rectification technology or multi-level technology. Multi pulse rectifier technology [4], that is, through the rectifier technology to make the harmonic current caused or emitted by the device smaller; multi-level converter technology, that is, using multi-level technology [5], to make the square wave current superimposed, so that it is closer to the sine wave, and the same as the voltage phase. The design is complex and the cost is high. Passive control method is to suppress the generated harmonics by means of passive filter and active filter. Passive filter [6] can only filter out the harmonics of specific frequency, and its volume and weight are large. The filtering effect is easily affected by the component parameter drift and the impedance change of aviation power supply. Active power filter (APF) is a kind of equipment which can dynamically compensate harmonics and improve power quality. APF has adaptive function. When the harmonic or reactive power changes in the power system, APF can detect the change in time and track the harmonic or reactive current with opposite output direction and equal size. It can be seen that APF is a good measure to solve the problem of harmonic pollution in aircraft power system and improve the power quality of aircraft equipment.

In order to solve the problem of harmonics, a three-level active filter which can dynamically compensate harmonics and has adaptive function is selected. In this paper, an improved rife algorithm is proposed to detect the frequency of variable frequency power supply in aviation, so that the detection accuracy will not be affected when noise occurs. In order to improve the detection accuracy of harmonic current, detection method without detecting the voltage of aviation power supply is selected to detect harmonic cur-rent. In order to meet the requirements of the harmonic compensation effect of the aviation variable frequency power supply system, this paper proposes a quasi-proportional resonant controller based on the selected pre-corrected Tustin transformation method. Compared with the proportional resonant controller, it can reduce the system sensitivity, increase the bandwidth, adapt to the small range of frequency fluctuations at the resonant frequency, and be conducive to the stable operation of the system and the realization of digital control.

II. MATHEMATICAL MODEL OF THREE-PHASE FOUR WIRE NPC THREE-LEVEL ACTIVE FILTER

It can be divided into two-level, three-level and multi-level categories according to the number of main circuit topological levels adopted by active filter. Compared with two-level APF, three-level APF has lower voltage stress under the same conditions, which is suitable for high-power ap-plications, and is conducive to reducing switching frequency and harmonics. The three-level topology for the three-phase four wire system can be divided into two types: three-level arm and four-bridge arm. The three-level topology is not as good as the four-bridge arm in the ability of zero sequence current compensation. However, compared with the four-bridge arm, the three-bridge arm topology has fewer switches, simpler control and lower cost. Therefore, the three-level three bridge arm topology is selected in this paper.

The diode clamped three-level topology (three bridge arm) is shown in the figure below.

The premise that APF can compensate har-monic current accurately and effectively is to establish the correct mathematical model. In or-der to facilitate the analysis, it is usually necessary to transform the model of APF from three-phase static coordinate system to synchronous rotating coordinate system. At the same time, because of the three-phase four wire system, we need to consider the influence of zero sequence component on the system, so we can choose the rotation coordinate system to control the zero-sequence component.

The relationship between the three-phase static coordinate system and the rotating coordinate system is as follows:

$$\begin{cases} X_{dq0} = T_{abc-dq0}(\theta)X_{abc} \\ X_{abc} = T_{abc-dq0}(\theta)^{-1}X_{dq0} \end{cases} \tag{1}$$

In this paper, the output current i_{cj} and output terminal voltage u_{jo} of aviation power supply, switch functions S_{ju}, S_{jd} and APF are converted to $dq0$ coordinate system by constant power conversion, and the three-phase four wire APF mathematical model is converted to $dq0$ coordinate system as follows:

$$\begin{cases} L \cdot \dfrac{di_{cd}}{dt} = -R \cdot i_{cd} + \omega L i_{cq} - (S_{du}u_{dcu} - S_{dd}u_{dcd}) + u_{sd} \\ L \cdot \dfrac{di_{cq}}{dt} = -R \cdot i_{cq} - \omega L i_{cd} - (S_{qu}u_{dcu} - S_{qd}u_{dcd}) + u_{sq} \\ L \cdot \dfrac{di_{c0}}{dt} = -R \cdot i_{c0} - (S_{qu}u_{dcu} - S_{qd}u_{dcd}) + u_{s0} \\ C_d \dfrac{du_{dcu}}{dt} = i_{du} = S_{du}i_{cd} + S_{qu}i_{cq} + S_{0u}i_{c0} \\ C_d \dfrac{du_{dcd}}{dt} = -i_{dd} = -S_{dd}i_{cd} - S_{qd}i_{cq} - S_{0d}i_{c0} \end{cases}$$

$$\tag{2}$$

It can be seen from the formula that there is coupling between d axis current and q axis current in $dq0$ coordinate system, and zero axis current is not coupled with d and q axis current. By comparing the mathematical models of APF in and $dq0$ coordinates, it is found that the latter is similar except for the current coupling in d and q axes.

III. RESEARCH ON THE DETECTION ALGORITHM OF FREQUENCY AND HARMONIC CURRENT IN AVIATION FREQUENCY CONVERSION POWER SUPPLY SYSTEM
A. FREQUENCY DETECTION METHOD OF AVIATION VARIABLE FREQUENCY POWER SUPPLY SYSTEM
The application of APF device in this paper is air frequency conversion AC power system, its frequency range

is 360Hz-800Hz. When the active filter is used to control the harmonics, the frequency of the aviation variable frequency power supply must be determined first, then the coordinate transformation and the calculation and control of the harmonic current can be carried out. Therefore, the frequency detection of the aviation variable frequency power supply is particularly important.

Two-line amplitude method (Rife method) [16] is improved on the basis of DFT maximum spectrum direct frequency measurement method, which improves the frequency detection accuracy and execution rate, but when the frequency of the measured signal is close to the maximum spectrum frequency, it is easy to produce large errors. In this paper, an improved rife algorithm is proposed, which makes the detection accuracy unaffected when noise appears.

$(k + 1/3, k + 2/3)$ region is defined as the middle position of k and $k + 1$. When rife algorithm is used to detect the frequency, whether the frequency is in the middle position of the two spectral lines is determined. If it is, the detection result will be the result of Rife algorithm; if not, it will be modified. The modified method is to shift the frequency of the measured signal, so that the measured signal is always in the middle position, then the accuracy of the frequency detection results will be improved.

Suppose the Rife algorithm detection result is f_r, because $|X_{k_0}| > |X_{k_0+\alpha}|$, there is $|f_r - k_0/Nf_s| \le 1/2\Delta f$. If $1/3\Delta f < |f_r - k_0/Nf_s| < 1/2\Delta f$ is met, f_r is the test result. If not, set the frequency shift of the measured signal as δ_k, as follows:

$$\delta_k = \frac{1}{2} - \frac{|X_{k_0+\alpha}|}{|X_{k_0}| + |X_{k_0+\alpha}|} \qquad (3)$$

The new spectrum after frequency shift is:

$$X'(k) = \sum_{n=0}^{N-1} X(k - \alpha\delta_k), \qquad k = 0, 1, \cdots, N - 1 \quad (4)$$

The frequency formula of the improved Rife method after frequency shift is obtained as follows:

$$\hat{f}_0 = \frac{f_s}{N} \cdot (k_0 - \alpha\delta_k + \frac{\alpha \cdot |X_{k_0-\alpha\delta_k+\alpha}|}{|X_{k_0-\alpha\delta_k+\alpha}| + |X_{k_0-\alpha\delta_k}|}) \quad (5)$$

In the above formula $\alpha = \pm 1$, when $|X_{k_0+1}| > |X_{k_0-1}|$, $\alpha = 1$. When $|X_{k_0+1}| \le |X_{k_0-1}|$, $\alpha = -1$. Because when the improved rife method is used to detect the signal frequency, the frequency of the measured signal will always be shifted to the middle of the spectral line, and then the rife method is used to detect the signal frequency, so the detection accuracy is high.

Therefore, the algorithm block diagram of frequency detection using the improved Rife method is as follows:

Table 1 shows the simulation results of power frequency detection with improved Rife algorithm when the power frequency is 400, 600 and 800Hz respectively, and the detection error is kept within 0.5Hz. The power phase voltage is 115V, the frequency range is 360-800Hz, the sampling frequency is 20kHz, and the FFT points are 200.

TABLE 1. Simulation results of power frequency detection by improved Rife method.

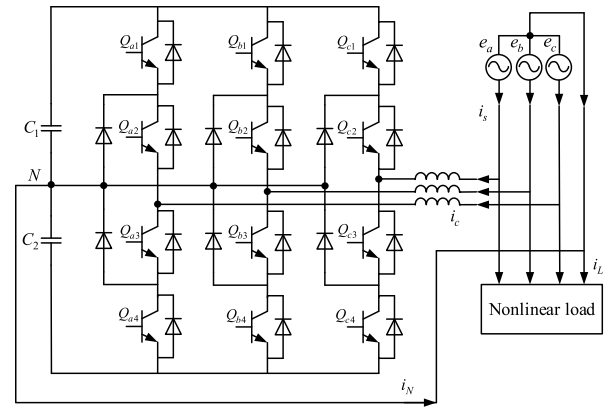| Given frequency	400Hz	600Hz	800Hz
Improved Rife method	399.9Hz	599.83Hz	799.92Hz

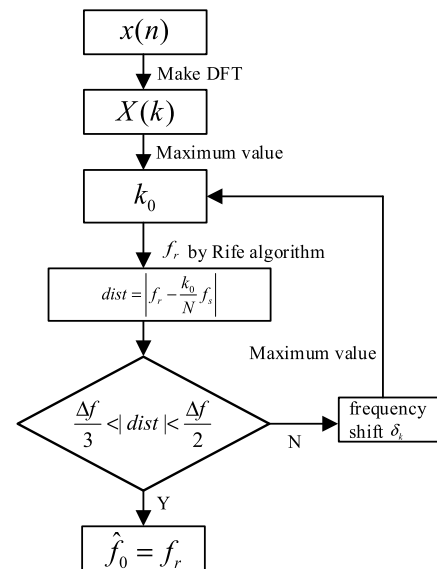**FIGURE 1.** Topology of three-level active power filter.

FIGURE 2. Algorithm block diagram of improved Rife method for frequency detection.

Take a frequency from 400Hz to 420Hz for detailed detection, and the results are as follows:

It can be seen from the above data that the detection error of the improved rife algorithm at each frequency point is less than ± 0.5Hz.

In case of step mutation from 400Hz to 420Hz, the test results are shown in Figure 3. The initial frequency of the power supply is 400Hz, which suddenly changes to 420Hz at 0.12s, and the delay of detection frequency is about 4ms. At the same time, there is no oscillation in the process of frequency mutation, and the steady-state error is maintained within 0.5Hz.
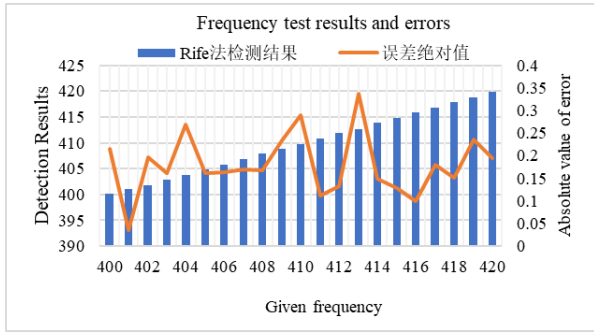
FIGURE 3. Test results and errors in frequency range from 400Hz to 420Hz.
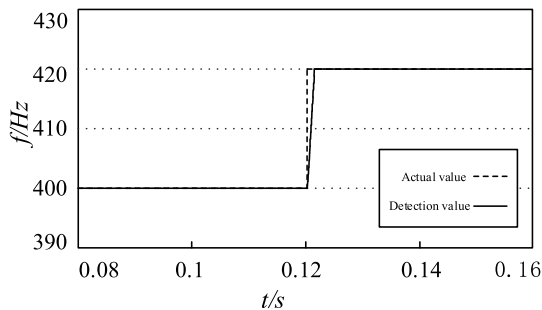

FIGURE 4. Simulation test results of 400Hz sudden change to 420Hz.

From the above data, it can be seen that the frequency detection error of the improved rife method does not exceed ±0.5Hz, and according to the national military standard GJB_181B-2012, the steady-state frequency range of 400Hz is 393-407Hz (±7Hz), so the accuracy of 0.5Hz can be used for the frequency detection under the aviation frequency conversion system.

B. DETECTION METHOD OF HARMONIC CURRENT IN AIR FRE QUENCY CONVERSION POWER SUPPLY SYSTEM

Due to the influence of nonlinear load and power frequency variation, harmonic current detection is the key point of APF to effectively compensate the harmonics in aviation power system.

The method based on instantaneous reactive power has good real-time performance and high detection accuracy [13]. It is widely used in active power filter, and can detect reactive power and harmonic current in real time. The traditional power calculation is defined by the average value, which is mainly suitable for the sine of voltage and current waveform. The instantaneous reactive power law defines the power from the instantaneous value, which can be used in non-sinusoidal or transitional situations.

The expressions of instantaneous active power and reactive power are as follows:

$$\begin{cases} p = e_a i_a + e_b i_b + e_c i_c \\ q = \dfrac{1}{\sqrt{3}}[(e_b - e_c)i_a + (e_c - e_a)i_b + (e_a - e_b)i_c] \end{cases} \quad (6)$$

The principle block diagram of $i_p - i_q$ detection method is shown in Figure 5. This method does not need to detect the
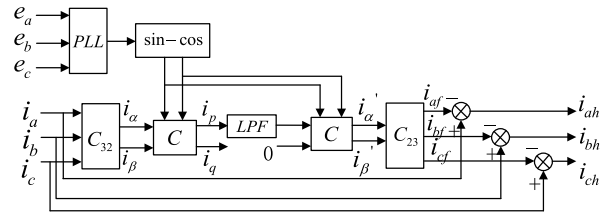

FIGURE 5. Principle block diagram of detection method $i_p - i_q$.

voltage of aviation power supply, so it is not affected by the voltage distortion of aviation power supply. Firstly, the detection current is transformed from *abc* coordinate system to $\alpha\beta$ coordinate system by coordinate transformation, and then the voltage of aviation power supply is locked. The phase-locked output is the voltage phase of the aviation power supply. The instantaneous active current i_p and the instantaneous reactive current i_q are calculated by the obtained phase and the sine cosine transformation matrix C. The matrix formula of sine cosine transformation is as follows:

$$C = C^{-1} = \begin{bmatrix} \sin \omega t & -\cos \omega t \\ -\cos \omega t & -\sin \omega t \end{bmatrix} \quad (7)$$

The calculated expressions of and are as follows:

$$\begin{bmatrix} i_p \\ i_q \end{bmatrix} = C \begin{bmatrix} i_\alpha \\ i_\beta \end{bmatrix} = CC_{32} \begin{bmatrix} i_a \\ i_b \\ i_c \end{bmatrix} \quad (8)$$

In practical application, the voltage of aviation power supply cannot be completely symmetrical. When the three-phase voltage of aviation power supply is asymmetrical, the following analysis can be made.

The symmetrical component method is used to decompose the three-phase voltage into positive sequence, negative sequence and zero sequence components. As follows:

$$e_m = e_m^+ + e_m^- + e_m^0 \quad (9)$$

In the above formula, $m = a, b, c$, where e_m^+ is the positive sequence component of voltage, e_m^- is the negative sequence component of voltage, and e_m^0 is the zero sequence component of voltage. By transforming the above formula, the expression of voltage positive sequence component is obtained as follows:

$$\begin{bmatrix} e_a^+ \\ e_b^+ \\ e_c^+ \end{bmatrix} = \frac{1}{3} \left\{ \begin{bmatrix} 1 & -\dfrac{1}{2} & -\dfrac{1}{2} \\ -\dfrac{1}{2} & 1 & -\dfrac{1}{2} \\ -\dfrac{1}{2} & -\dfrac{1}{2} & 1 \end{bmatrix} - j \begin{bmatrix} 0 & -\dfrac{\sqrt{3}}{2} & \dfrac{\sqrt{3}}{2} \\ \dfrac{\sqrt{3}}{2} & 0 & -\dfrac{\sqrt{3}}{2} \\ -\dfrac{\sqrt{3}}{2} & \dfrac{\sqrt{3}}{2} & 0 \end{bmatrix} \right\} \begin{bmatrix} e_a \\ e_b \\ e_c \end{bmatrix} \quad (10)$$

It can be seen from the above formula that there is a phase difference between the positive sequence components e_j^+ and $e_j (j = a, b, c)$ of each phase voltage. The output phase of PLL used in $i_p - i_q$ detection method is ωt, which is the phase of e_a. However, in the detection process, the desired correct phase should be in phase with e_a^+, so there is an error between the ωt obtained by phase-locked and the theoretical value. If the error is δ, the actual phase should be $(\omega t + \delta)$.

Suppose that the three-phase current expression is as follows:

$$i_m = i_m^+ + i_m^- + i_m^0 \qquad (11)$$

In the above formula, $m = a, b, c$, where $i_j^+ (j = a, b, c)$ is the positive sequence component of each phase current, i_j^- is the negative sequence component of each phase current, i_j^0 is the zero sequence component of each phase current, and $i_a^0 = i_b^0 = i_c^0 = (i_a + i_b + i_c)/3$.

It can be divided into the form of each harmonic and substituted into the above formula to get:

$$\begin{bmatrix} i_p \\ i_q \end{bmatrix} = \sqrt{3} \begin{bmatrix} \sum_{n=1}^{\infty} \begin{Bmatrix} I_n^+ \cos[(n-1)\omega t + \varphi_n^+ - \delta] \\ -I_n^- \cos[(n+1)\omega t + \varphi_n^- + \delta] \end{Bmatrix} \\ \sum_{n=1}^{\infty} \begin{Bmatrix} -I_n^+ \sin[(n-1)\omega t + \varphi_n^+ - \delta] \\ -I_n^- \sin[(n+1)\omega t + \varphi_n^- + \delta] \end{Bmatrix} \end{bmatrix} \qquad (12)$$

It can be seen from the formula that after coordinate transformation, the positive sequence components of each frequency current in the three-phase static coordinate system become $(n-1)\omega$, and the negative sequence current becomes $(n+1)\omega$. That is to say, the DC component is completely composed of fundamental positive sequence current.

The calculated i_p and i_q are filtered to obtain DC component:

$$\begin{bmatrix} \bar{i}_p \\ \bar{i}_q \end{bmatrix} = \begin{bmatrix} \sqrt{3}I_1^+ \cos(\varphi_1^+ - \delta) \\ -\sqrt{3}I_1^+ \sin(\varphi_1^+ - \delta) \end{bmatrix} \qquad (13)$$

Invert the DC component to obtain the fundamental positive sequence current in coordinate system:

$$\begin{bmatrix} i_{af}^+ \\ i_{bf}^+ \\ i_{cf}^+ \end{bmatrix} = C_{23}C^{-1} \begin{bmatrix} \bar{i}_p \\ \bar{i}_q \end{bmatrix} = \begin{bmatrix} \sqrt{2}I_1^+ \sin(\omega t + \varphi_1^+) \\ \sqrt{2}I_1^+ \sin\left(\omega t - \frac{2\pi}{3} + \varphi_1^+\right) \\ \sqrt{2}I_1^+ \sin\left(\omega t + \frac{2\pi}{3} + \varphi_1^+\right) \end{bmatrix} \qquad (14)$$

It can be seen from the above formula that in the case of voltage asymmetry of aviation power supply, the correct positive sequence component of fundamental wave detected is independent of the phase error δ caused by voltage asymmetry. Therefore, in the case of voltage distortion and three-phase asymmetry, the $i_p - i_q$ detection method can correctly detect the harmonic current.

The nonlinear load module is adopted, three-phase uncontrolled rectifier bridge is used, and the resistance is connected at the back of the bridge. At the same time, the three-phase
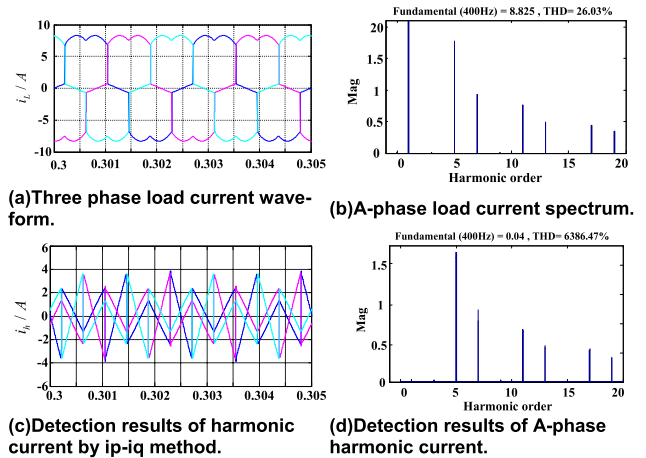

(a) Three phase load current waveform.

(b) A-phase load current spectrum.

(c) Detection results of harmonic current by ip-iq method.

(d) Detection results of A-phase harmonic current.

FIGURE 6. Waveform of load current and harmonic current detection results when power frequency is 400Hz.

TABLE 2. FFT analysis of load current and detected harmonic cur-rent when power frequency is 400Hz.

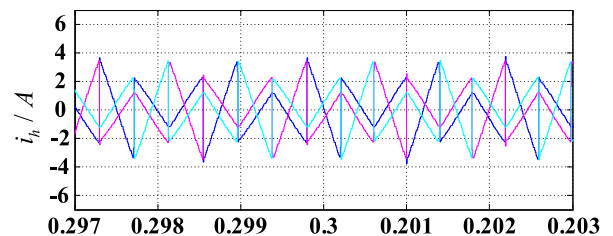| Harmonic number	5	7	11	13	17	19
Load current /A	1.69	0.84	0.68	0.48	0.42	0.34
Detection result /A	1.7	0.83	0.69	0.47	0.43	0.33
Error /A	0.01	-0.01	0.01	-0.01	0.01	-0.01

FIGURE 7. Detection waveform of harmonic current when power frequency changes from 400Hz to 420Hz.

parallel resistance is connected with the central line, where the resistance R is 40 Ω, R2, R3 and R4 are 120 Ω. When the power frequency is equal to 400Hz, the three-phase load current waveform is as shown in Figure 6 (a), and the THD content is 26.03%; the three-phase harmonic current detected by $i_p - i_q$ method based on instantaneous reactive power method is as shown in Figure 6 (c).

The following table shows the content of each frequency harmonic current in FFT analysis of load current and detected harmonic current:

It can be seen from the table that the absolute value of the error between the harmonic current detected by $i_p - i_q$ method based on the instantaneous reactive power method and the harmonic current actually contained is not more than 0.01A, the error is small and the detection accuracy is high.

When the frequency changes abruptly, the initial frequency is set to 400Hz, and it changes abruptly to 420Hz at 0.3s.

The harmonic current detection waveform at this time is shown in Figure 7. It can be seen from the figure that although the detection result will be delayed when the frequency changes, the detected harmonic current does not oscillate and changes smoothly when the frequency changes. FFT analysis of the load current and the detected harmonic current after the frequency mutation is carried out, and the error between the detection results of each harmonic and the actual value is also kept within 0.01A. This shows that the detection method based on the instantaneous reactive power theory is suitable for the situation that the power frequency changes in the range of 360-800Hz.

FIGURE 8. Bode diagram of PR control.

IV. RESEARCH ON CURRENT LOOP TRACKING CONTROL STRATEGY OF APF FOR AVIATION VARIABLE FREQUENCY POWER SUPPLY

After the accurate detection of frequency and harmonic current, the current command signal is obtained by calculation. The performance of the current tracking control link is directly related to the harmonic compensation effect of the aviation variable frequency power system. Three-level APF often uses a double closed-loop control structure that combines a voltage outer loop and a current inner loop. The current inner loop mainly realizes the non-static difference tracking of the command current, and the voltage outer loop function is to maintain the stability of the APF DC side voltage. This article is mainly aimed at the particularity of aviation variable frequency power system, and design and select the quasi-PR controller based on the pre-modified Tustin transform method.

A. CONTROL STRATEGY ANALYSIS AND COMPARISON

Resonance control is a control method based on internal model control principle. The internal model principle points out that if the closed-loop system can track the given signal without static error, it needs to include the *s*- domain model of the given signal in the open-loop system. Especially for the control of single-phase inverter, the given signal is AC signal, and in general, the control object does not contain the *s*- domain model of AC signal, so it is necessary to add the model of AC signal in the control system. The *s* model of AC signal is $s/(s^2+\omega^2)$, which is exactly a resonance control link. By implanting the AC signal model in the open-loop control system, the infinite gain can be achieved at the specified frequency point, so that the AC signal can be tracked without static error. The resonance controller has large gain and narrow band at the specified frequency point. It is very sensitive to the frequency change of AC signal and easy to cause system oscillation. Therefore, the quasi resonant controller is proposed to reduce the gain at the resonant point and improve the bandwidth of the resonant point.

1) ANALYSIS OF PROPORTIONAL RESONANCE CONTROLLER

The internal model principle points out that in order to make the system track the given signal perfectly, it is necessary to include the signal model in the frequency domain of the
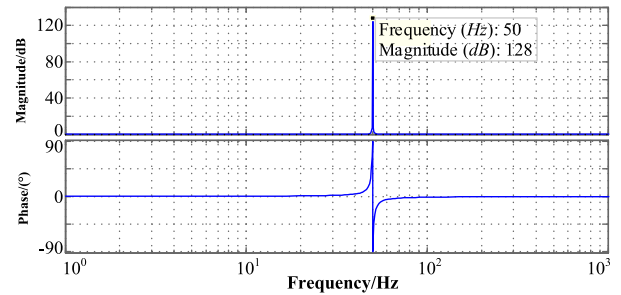
system. In order to track the AC signal without static error, it is necessary to include the frequency domain model of the AC signal in the system model. The frequency-domain model of AC signal is just a resonant link, so a proportional resonant controller (PR controller) is proposed as the controller.

The model of AC signal is put into the system controller to increase the open-loop gain of the system at the specified frequency point, enhance the signal at the specified frequency point, which is conducive to the regulation of the system. The resonant link is a typical two order linear- integrator, which can be analyzed by the existing linear theory. In order to enhance the dynamic response and anti-interference ability of the resonance link, the proportional resonance controller is generally composed of the resonance link and the proportional link. Its transfer function is as follows:

$$G_{PR}(s) = K_P + \frac{2K_R s}{s^2 + \omega_0^2} \tag{15}$$

where, K_P is the proportion coefficient, K_R is the resonance coefficient and ω_0 is the resonance frequency. Figure 8 is a Bode diagram of proportional resonance. Among them, $K_P = 1, K_R = 5, \omega_0 = 100\pi$.

It can be seen from the Bode diagram that the gain of PR controller at the resonance point ω 0 is almost infinite, and the gain at other frequencies is 0, so it can track the AC signal at the resonance frequency without static difference. However, in the variable frequency power supply, even if the fundamental frequency of the power supply is detected, the detection results will have errors within the allowable range; in the steady-state situation, the actual frequency of the power supply will also have fluctuations within the allowable range. However, PR controller has large gain and narrow bandwidth at resonance point, so it has poor adaptability to frequency change and poor anti disturbance ability, which easily leads to system instability. At the same time, due to the influence of digital control on the accuracy, it is not easy to adjust to the resonance point for control. Therefore, it needs to be improved to reduce the sensitivity and high gain characteristics at the resonance frequency, so as to facilitate the realization of the system. PR can be improved to quasi proportional resonance (QPR) control.
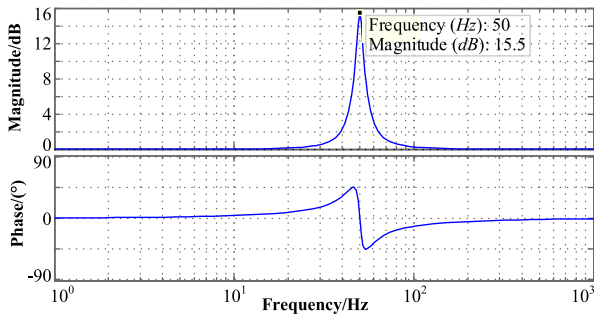
FIGURE 9. Bode diagram of quasi PR control.

FIGURE 10. Principle block diagram of current loop with quasi PR controller.

2) ANALYSIS OF QUASI PROPORTIONAL RESONANCE CONTROLLER

The first-order high gain and low-pass filter is added to the PR controller to ensure the high gain at the resonance point, at the same time, the bandwidth of the controller is increased, and the sensitivity of the system is reduced. This is the quasi-proportional resonance controller, whose transfer function is as follows (15):

$$G_{PR}(s) = K_P + \frac{2K_R\omega_c s}{s^2 + 2\omega_c s + \omega_0^2} \quad (16)$$

where ω_0 is the cut-off frequency. The Bode diagram of quasi proportional resonance controller is shown in Figure 9.

From equation (15), it can be seen that the gain of quasi PR controller at ω_0 is $K_P + K_R$. Although $K_P + K_R$ is a finite value different from PR controller, the gain can meet the requirements by adjusting resonance parameters, so that the steady-state error is 0. On the other hand, compared with the PR controller before the improvement, the bandwidth of the controller increases significantly after the EEE is added, which can adapt to the small range frequency fluctuation at the resonance frequency, and is conducive to the stable operation of the system and the realization of digital control. QPR control retains the characteristic of PR control without static error at the fundamental wave, enhances the anti-interference ability and improves the overall performance of the controller.

Figure 9 is a Bode diagram of quasi proportional resonance. Among them, $K_P = 1$, $K_R = 5$, $\omega_0 = 100\pi$, $\omega_c = 10$.

It can be seen from Figure 9 that, compared with the proportional resonance control, the gain of the quasi proportional resonance control at the resonance point decreases, but it is also sufficient to meet the requirements of tracking without static difference. At the same time, the band-width increases, allowing the frequency to fluctuate in a small range, which is conducive to the realization of digital control. The increase of the phase angle margin of the quasi proportional resonant controller is beneficial to the stable operation of the system.

3) CURRENT LOOP WITH QUASI PROPORTIONAL RESONANT CONTROLLER

The PR controller has infinite gain at the resonance frequency, and the gain at the non-resonance frequency is
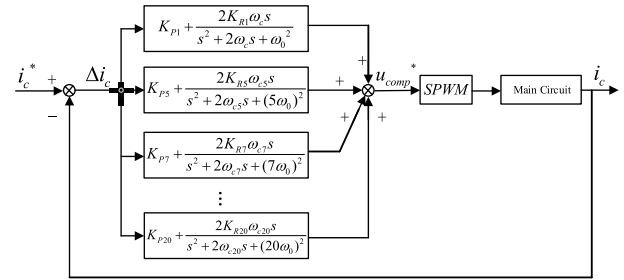
approximately 0. It has the function of automatically screening the frequency, so it is suitable for frequency division control of harmonic current. For an APF in an aeronautical variable frequency power supply system, its current loop needs to be provided with multiple quasi-proportional resonance controllers with different resonance frequencies, and each resonance frequency is the same as the harmonic frequency in the load current. Aviation power is a three-phase four-wire system, so the harmonic is $6k \pm 1$ frequency, where k is a positive integer. The principle block diagram of the current loop using a quasi-proportional resonant controller is shown in Figure 8 below.

In Figure 10, i_c^* is the calculated harmonic reference current, i_c is the actual current output by the APF, and Δi_c is the difference between the reference command current and the APF actual output current. The input of the PR controller for each frequency is the difference Δi_c between the command current and the actual out-put current. Because for the harmonic current, as the frequency increases, its amplitude will also decrease accordingly. Therefore, in practical ap-plications, only harmonics within 20 times are generally compensated. Among them, ω_0 is the fundamental frequency. Considering the existence of the voltage outer loop, it is necessary to maintain the stability of the APF DC side voltage, so the fundamental current loop is required. When the fundamental frequency of the aeronautical variable frequency power supply changes, the real-time frequency is transmitted to the quasi-PR controller in time through the above frequency detection method, and the harmonic cur-rent resonance frequency of ω_0 and the following will also change accordingly. The sum of the current loop output of the quasi-PR controller of each frequency is added, that is, u_{comp} is the modulation voltage, which is input to the subsequent modulation link, and the driving signal of the switching device in the main circuit can be obtained.

From Figure 8, the transfer function of the current controller is:

$$G_{PR}(s) = \sum_{k=1,5,7,\cdots} K_{iP} + \frac{2K_{iR}\omega_{ci} s}{s^2 + 2\omega_{ci} s + (i\omega_0)^2} \quad (17)$$

B. IMPLEMENTATION OF QUASI-PROPORTIONAL RESONANCE CONTROLLER

The fundamental frequency range of aviation variable frequency power supply is 360-800Hz. When the fundamental
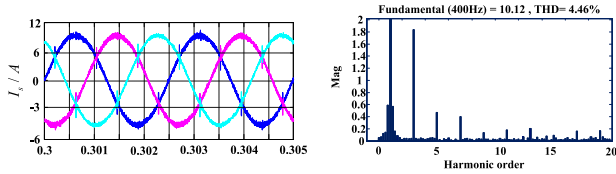
(a) Current waveform of three-phase power supply after compensation.

(b) A-phase power supply current spectrum.

FIGURE 11. Power current waveform after compensation when power frequency is 400Hz.

(a) Current waveform of three-phase power supply.

(b) Spectrum when power frequency is 400Hz.

(c) Spectrum when power frequency is 410Hz.

FIGURE 12. Compensation effect when power frequency changes from 400Hz to 410Hz.

frequency of the power supply is high, the harmonic frequency generated on this basis will be higher. Therefore, the method of discretization of the resonance frequency needs to be selected. In this paper, a pre-modified Tustin transform method is chosen to align the PR controller for discrete design.

The pre-modified Tustin transform is as follows:

$$s = \frac{\omega}{\tan(\omega T_s/2)} \cdot \frac{z-1}{z+1} \qquad (18)$$

Among them, T_s is the sampling period.

The transfer function of the quasi-PR controller in the z domain is as follows:

$$s = \frac{\omega}{\tan(\omega T_s/2)} \cdot \frac{z-1}{z+1} \qquad (19)$$

Among them: $b_0 = \frac{2\omega_c C K_R}{C^2 + 2\omega_c C + \omega_i^2} + K_P$, $b_1 = \frac{(2\omega_i^2 - 2C^2)K_P}{C^2 + 2\omega_c C + \omega_i^2}$, $b_2 = \frac{K_P(C^2 - 2\omega_c C + \omega_i^2) - 2K_R\omega_c C}{C^2 + 2\omega_c C + \omega_i^2}$, $a_1 = \frac{2\omega_i^2 - 2C^2}{C^2 + 2\omega_c C + \omega_i^2}$, $a_2 = \frac{C^2 - 2\omega_c C + \omega_i^2}{C^2 + 2\omega_c C + \omega_i^2}$, $C = \frac{\omega_i}{\tan(\omega_i T_s/2)}$:

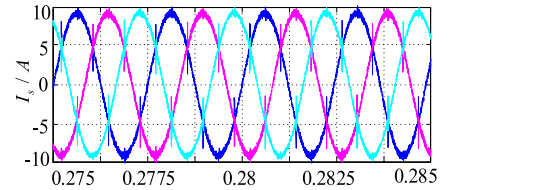The corresponding difference equation is derived as:

$$y(k) = b_0 x(k) + b_1 x(k-1) + b_2 x(k-2)$$
$$- a_1 y(k-1) - a_2 y(k-2) \qquad (20)$$

In formula (19), $y(k)$ is the output signal of the quasi-PR controller, and $x(k)$ is the input signal of the quasi-PR controller.

C. CURRENT LOOP SIMULATION BASED ON QUASI-PR CONTROLLER

When the power frequency is 400Hz, after the active filter compensation, the power supply current I_s waveform at this time is as shown in Figure 11. The THD of the three phases after compensation are 4.46%, 4.55%, and 4.52%. It meets the requirements of the national military standard GJB_181B-2012 aircraft power supply characteristics, that is, the current THD is less than 10%. Among them, in the current loop quasi-PR controller, the current inner loop proportion parameter K_p is selected as 200, the current inner loop resonance parameter K_R is selected as 500, and the cutoff frequency is selected as 5.

When the aircraft power frequency changes suddenly, check the harmonic compensation effect at this time. Set at 0.28s, the power frequency abruptly changes from 400Hz to
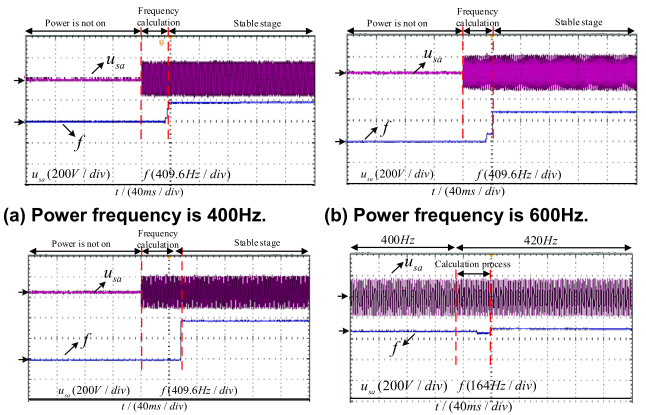
(a) Power frequency is 400Hz.

(b) Power frequency is 600Hz.

(c) Power frequency is 800Hz.

(d) Power frequency changes from 400Hz to 420Hz.

FIGURE 13. Frequency test results at different power frequencies.

410Hz. At this time, the power current harmonic compensation result is shown in Figure 12 below.

V. EXPERIMENTAL RESULTS

In order to verify the above theory, an APF experimental platform was set up to verify the frequency and harmonic current detection algorithms and PR control strategies. A three-phase programmable AC source was used as the input three-phase AC power. The phase voltage was set to 115V and the frequency range was set. 360-800Hz. Non-linear load consists of three-phase uncontrolled rectifier bridge and resistor.

A. EXPERIMENTAL VERIFICATION OF FREQUENCY DETECTION ALGORITHM

First, set the power frequency to 400Hz, 600Hz, and 800Hz respectively. The waveform of stable output from power supply to frequency detection result is shown in Figure 13 below. It can be seen from the figure that it takes a certain time to stabilize the output frequency calculation result, which is about 40ms. This time mainly includes the time for initial sampling and calculation of the signal when the power supply

TABLE 3. Test results of power frequency detection by improved Rife method.

Given frequency	400Hz	420Hz	600Hz	800Hz
Improved Rife method	400.41Hz	420.26Hz	600.21Hz	799.71Hz

(a) Load current and detected harmonic current waveform.

(b) Load current spectrum.

(c) Detected harmonic current spectrum.
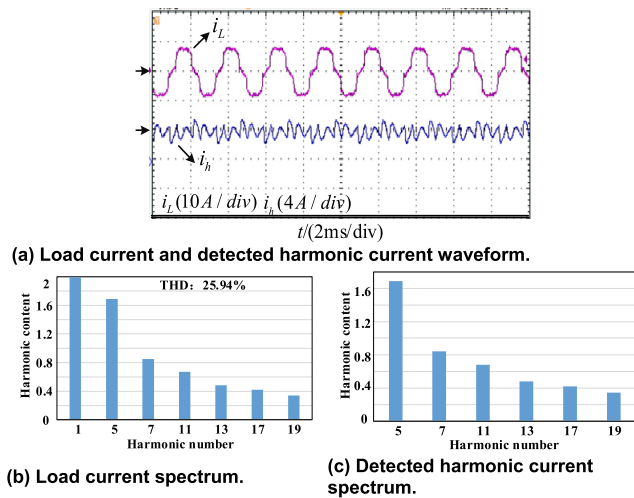
FIGURE 14. Load current and its spectrum when the power frequency is 400Hz.

(a) Load current and detected harmonic current waveform.

(b) Detected harmonic current spectrum.

FIGURE 15. Test results of load current and harmonic when power frequency is 600Hz.

(a) Load current and detected harmonic current waveform

(b) Detected harmonic current spectrum

FIGURE 16. Test results of load current and harmonic when power frequency is 800Hz.

(a) Power supply current waveform without or with compensation when the frequency is 400Hz.

(b) Power supply current waveform without or with compensation when the frequency is 600Hz.

(c) Power supply current waveform without or with compensation when the frequency is 800Hz.

FIGURE 17. Power supply current waveform before and after compensation of each frequency point.

is just powered. Figure 13 (d) is the waveform of the detection result when the power frequency changes from 400Hz to 420Hz. It can be seen from the figure that after the frequency changes, the time required to accurately calculate the new frequency is about 50ms.

The specific detection results of each frequency point in Figure 11 are shown in Table 3. It can be seen that the detection error is within ±0.5Hz. The experimental results are similar to the simulation. According to the national military standard GJB_181B-2012, it can be known that the steady-state frequency range of 400Hz is: 393-407Hz (±7Hz), so the accuracy of 0.5Hz can be used for frequency detection in the aviation frequency conversion system.

B. EXPERIMENTAL VERIFICATION OF HARMONIC CURRENT DETECTION METHOD

When the power frequency is 400Hz, taking the phase A as an example, the load current waveform and the detected harmonic current waveform are shown in Figure 14 (a). FFT analysis of the load current waveform shows that the load current THD is 25.94%. It can be known from Figure 14 (b) (c) that when the power sup-ply frequency is 400Hz, the error between the harmonic current detected by the method and the actual load current does not exceed 0.1A.

Next, set the power frequency to 600Hz and 800Hz respectively. The load current waveform and the detected harmonic current waveform are shown in the figure.

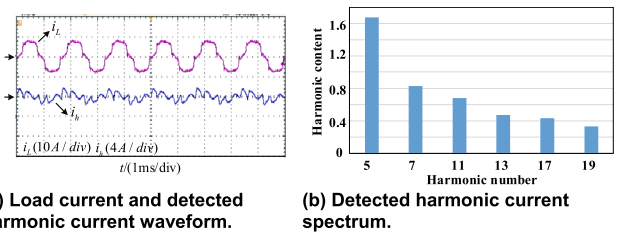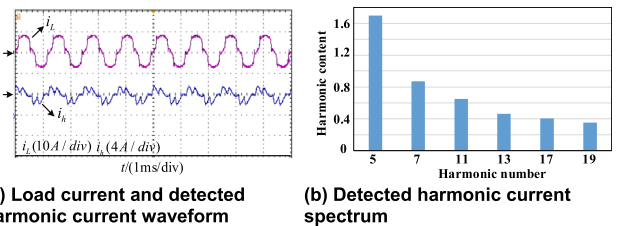Because when the power frequency changes and the load parameters remain unchanged, the change in frequency will not cause the current distortion coefficient to change, and the current THD is about 26%, so the load current spectrum at other frequencies is not given here. FFT analysis is performed on the harmonic current detected by the $i_p - i_q$ method, and it can be known that the error of the harmonic current content between the harmonic current detected at each frequency point and the actual load current does not exceed 0.1A.

C. EXPERIMENTAL VERIFICATION OF DUAL-LOOP CONTROL STRATEGY BASED ON QUASI-PR CONTROL

When the power frequency is 400Hz, 600Hz, 800Hz, taking the A phase as an example, the power supply current
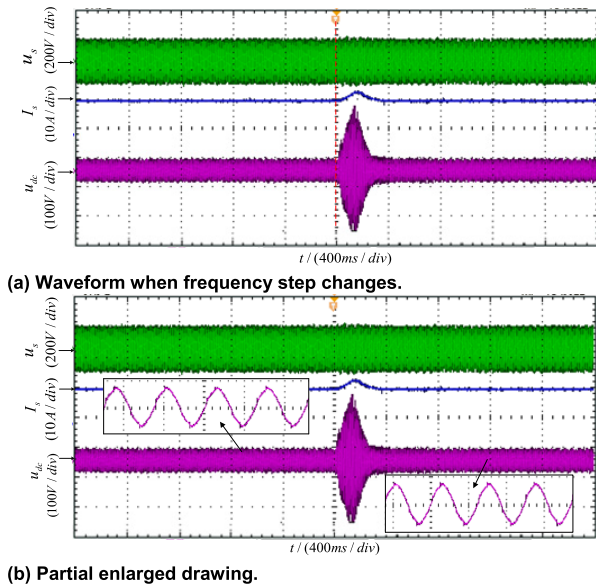
(a) Waveform when frequency step changes.

(b) Partial enlarged drawing.

FIGURE 18. Compensation waveform when power frequency changes from 400Hz step to 405Hz.

TABLE 4. Harmonic currents before and after current compensation of each frequency power supply (%).

Frequency	THD	5	7	11	13
Before compensation	26	1.70	0.85	0.66	0.49
400Hz	5.95	0.56	0.42	0.46	0.40
600Hz	6.01	0.57	0.43	0.49	0.41
800Hz	6.59	0.65	0.46	0.50	0.44

waveforms before and after compensation are as shown in Figure 17 below. In the experiment, the 5th, 7th, 11th, and 13th harmonics were selected to compensate. It can be seen from the figure that the power supply current at each frequency point has serious distortion and large harmonic content before compensation. After compensation, the harmonic content is reduced and the sine degree of waveform is higher. Table 4 shows the specific FFT analysis results of the power supply current before and after compensation. The current THD decreases significantly after harmonic compensation.

When the power frequency changes from 400Hz to 405Hz, the compensation effect is shown in Figure 18 below. It can be seen from the waveform diagram that when the frequency changes suddenly, the DC side voltage fluctuates by 50V, which causes the APF fundamental wave current loop to fluctuate, which causes the APF output current to generate a peak current when the frequency changes suddenly. The oscillation maintenance time is 0.2s. The maximum current spike is about 20A. When the DC-side voltage resumes stability again, the APF output current also stabilizes, which can be stably compensated, and the current THD after stabilization is 6.09%, which meets the requirements of the index.

According to the experimental results, it can be seen that after the APF compensation of the power supply current in

the aviation variable frequency power system, the THD is reduced to about 6%, and the power quality is significantly improved, which meets the requirement of THD less than 10% in the characteristics of aircraft power.
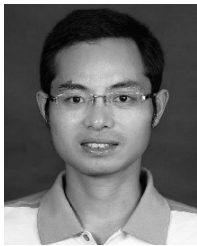
VI. CONCLUSIONS

This article mainly performs theoretical analysis and experimental verification on the three-level active filter suitable for aerospace variable frequency power system (115V/360-800Hz). The conclusions are as follow:

a. Improved Rife method based on DFT analysis for frequency detection with high detection accuracy, meeting the requirements of high frequency and wide variation range of aviation variable frequency power system;

b. Through harmonic current detection by detection method, the detection cur-rent result is basically consistent with the actual current waveform;

c. Experimental verification of the dual-loop control strategy based on quasi-PR resonance control has significantly improved the grid-connected current quality, and its THD meets the requirements of aircraft power characteristics in the National Army Standard.

REFERENCES

[1] Y. Yan and S. Xie, *Power Supply System of Civil Aviation Aircraft*. Beijing, China: Aviation Industry Press, 1995.

[2] J. A. Rosero, J. A. Ortega, E. Aldabas, and L. Romeral, "Moving towards a more electric aircraft," *IEEE Aerosp. Electron. Syst. Mag.*, vol. 22, no. 3, pp. 3–9, Mar. 2007.

[3] Z. Wang, J. Yang, and J. Liu, *Harmonic Suppression and Reactive Power Compensation*. Beijing, China: Mechanical Industry Press, 1998.

[4] S. Choi, B. S. Lee, and P. N. Enjeti, "New 24-pulse diode rectifier systems for utility interface of high-power AC motor drives," *IEEE Trans. Ind Appl.*, vol. 33, no. 2, pp. 531–537, Mar./Apr. 1997.

[5] J. Li, *Multilevel Converter Technology*. Beijing, China: Mechanical Industry Press, 1998, pp. 24–27.

[6] Y. Zhao and Q. Zhao, *Power System Harmonics*. Beijing, China: Mechanical Industry Press, 2009.

[7] B. M. Bird, J. F. Marsh, and P. R. Mclellan, "Harmonic reduction in multiple converters by triple-frequency current injection," *Proc. IEEE*, vol. 10, no. 16, pp. 1730–1734, 1969.

[8] H. Sasaki and T. Machida, "A new method to eliminate AC harmonic currents by magnetic flux compensation-considerations on basic design," *IEEE Trans. Power App. Syst.*, vol. PAS-90, no. 5, pp. 2009–2019, Sep. 1971.

[9] D. Chen, S. Xie, T. Guo, and B. Zhou, "Shunt active power filters applied in the aircraft power utility," in *Proc. IEEE 36th Conf. Power Electron. Spec.*, Jun. 2005, pp. 59–63.

[10] D. Chen, *Research on the Key Technology of Active Power Filter Applied to Aircraft AC Power System*. Nanjing, China: Nanjing Univ. Aeronautics and Astronautics, 2007.

[11] M. I. M. Montero, E. R. Cadaval, and F. B. Gonzalez, "Comparison of control strategies for shunt active power filters in three-phase four-wire systems," *IEEE Trans. Power Electron.*, vol. 22, no. 1, pp. 229–236, Jan. 2007.

[12] B. Singh, P. Jayaprakash, T. R. Somayajulu, D. P. Kothari, A. Chandra, and K. Al-Haddad, "Integrated three-leg VSC with a zig-zag transformer based three-phase four-wire DSTATCOM for power quality improvement," in *Proc. 34th Annu. Conf. IEEE Ind. Electron.*, Nov. 2008, pp. 796–801.

[13] Z. Wang and J. Liu, "Development of harmonic suppression and reactive power compensation technology for power electronic devices," *Power Electron. Technol.*, pp. 100–104, 1997.

[14] E. Lavopa, P. Zanchetta, M. Sumner, and F. Cupertino, "Real-time estimation of fundamental frequency and harmonics for active shunt power filters in aircraft electrical systems," *IEEE Trans. Ind. Electron.*, vol. 56, no. 8, pp. 2875–2884, Aug. 2009.

[15] Z. Qiu, "Research on control algorithm of three-phase four wire three-level APF," Univ. Electron. Sci. Technol., Chengdu, China, Tech. Rep., 2014.

[16] S. Kay, "A fast and accurate single frequency estimator," *IEEE Trans. Acoust., Speech, Signal Process.*, vol. 12, no. 37, pp. 1987–1990, Dec. 1989.

[17] Z. Shuquan *et al.*, "Specified subharmonic current control in multi synchronous rotating coordinate system," *Chin. J. Elect. Eng.*, 2010.

[18] J.-C. Wu and H.-L. Jou, "Simplified control method for the single-phase active power filter," *IEE Proc.-Electr. Power Appl.*, vol. 143, no. 3, pp. 219–224, May 1996.

[19] D. N. Zmood, D. G. Holmes, and G. H. Bode, "Frequency-domain analysis of three-phase linear current regulators," *IEEE Trans. Ind. Appl.*, vol. 37, no. 2, pp. 601–610, Mar./Apr. 2001.

[20] D. N. Zmood and D. G. Holmes, "Stationary frame current regulation of PWM inverters with zero steady-state error," *IEEE Trans. Power Electron.*, vol. 18, no. 3, pp. 814–822, May 2003.

[21] J. Shao, "Research on the method of harmonic current compensation in the power system of all electric aircraft," Xi'an Univ. Technol., Xi'an, China, Tech. Rep., 2009.

[22] Y. Lu, *Research on Active Power Filter Applied to Aircraft AC Power Supply*. Nanjing, China: Nanjing Univ. Aeronautics and Astronautics, 2009.

XINYING WANG graduated from Hainan University, in 2017, majoring in electrical engineering. She is currently pursuing the master's degree in electrical engineering from the Nanjing University of Aeronautics and Astronautics, China.

Her main research interest includes power electronic system integration.

ZHENYANG HAO (Member, IEEE) received the bachelor's degree in electrical engineering from Nanjing Normal University, in 2004, and the master's and Ph.D. degrees in power electronics and motion drive from the Nanjing University of Aeronautics and Astronautics, in 2010.

He has been an Associate Professor with the Department of Electrical Engineering, Nanjing University of Aeronautics and Astronautics, since 2013. His research interests include new energy power electronic conversion technology, aviation power supply and power actuator technology, electric vehicle motor design, and driving technology.

XIN CAO (Member, IEEE) received the B.Eng., M.Sc., and Ph.D. degrees in electrical engineering from the Nanjing University of Aeronautics and Astronautics, Nanjing, China, in 2003, 2006, and 2010, respectively.

Since 2011, he has been with the Nanjing University of Aeronautics and Astronautics. From June 2011 to September 2012, he was a Research Associate with the Department of Aeronautical and Automotive Engineering, Loughborough University, Loughborough, U.K. His current research interests include distributed generation and renewable energy, electric vehicles, switched reluctance motors, and magnetically levitated bearingless motors.

● ● ●